Moesin is required for HIV-1-induced CD4-CXCR4 interaction, F-actin redistribution, membrane fusion and viral infection in lymphocytes

Marta Barrero-Villar[1,*], José Román Cabrero[1,*], Mónica Gordón-Alonso[1], Jonathan Barroso-González[2], Susana Álvarez-Losada[3], M. Ángeles Muñoz-Fernández[3], Francisco Sánchez-Madrid[1,‡] and Agustín Valenzuela-Fernández[1,2]

[1]Servicio de Inmunología, Hospital Universitario de La Princesa, 28006 Madrid, Spain
[2]Departamento de Medicina Física y Farmacología, Facultad de Medicina, Universidad de La Laguna, 38071 Tenerife, Spain
[3]Servicio de Inmuno-Biología Molecular, Hospital General Universitario Gregorio Marañón, 28007 Madrid, Spain
*These authors contributed equally to this work
‡Author for correspondence (e-mail: fsanchez.hlpr@salud.madrid.org)

Accepted 6 October 2008
Journal of Cell Science 122, 103-113 Published by The Company of Biologists 2009
doi:10.1242/jcs.035873

Summary

The human immunodeficiency virus 1 (HIV-1) envelope regulates the initial attachment of viral particles to target cells through its association with CD4 and either CXCR4 or CCR5. Although F-actin is required for CD4 and CXCR4 redistribution, little is known about the molecular mechanisms underlying this fundamental process in HIV infection. Using $CD4^+$ $CXCR4^+$ permissive human leukemic CEM T cells and primary lymphocytes, we have investigated whether HIV-1 Env might promote viral entry and infection by activating ERM (ezrin-radixin-moesin) proteins to regulate F-actin reorganization and CD4/CXCR4 co-clustering. The interaction of the X4-tropic protein HIV-1 gp120 with CD4 augments ezrin and moesin phosphorylation in human permissive T cells, thereby regulating ezrin-moesin activation. Moreover, the association and clustering of CD4-CXCR4 induced by HIV-1 gp120 requires moesin-mediated anchoring of actin in the plasma membrane. Suppression of moesin expression with dominant-negative N-moesin or specific moesin silencing impedes reorganization of F-actin and HIV-1 entry and infection mediated by the HIV-1 envelope protein complex. Therefore, we propose that activated moesin promotes F-actin redistribution and CD4-CXCR4 clustering and is also required for efficient X4-tropic HIV-1 infection in permissive lymphocytes.

Supplementary material available online at
http://jcs.biologists.org/cgi/content/full/122/1/103/DC1

Key words: ERM, Ezrin-radixin-moesin, F-actin redistribution, CD4-CXCR4 interaction, HIV-1 infection and entry

Introduction

The entry of HIV into a target cell requires the interaction of multiple receptor and co-receptor molecules with each viral envelope (Env) trimer to promote the formation of fusion pores (Doms, 2000; Kuhmann et al., 2000). F-actin reassembly appears to be involved in Env-induced CD4, CXCR4 and LFA-1 redistribution to cell-cell junctions during viral spreading (Jolly et al., 2004), and drugs that affect actin dynamics appear to inhibit Env-mediated fusion (Eitzen, 2003; Pontow et al., 2004); but it is unclear whether these drugs affect HIV-1 Env activity (Campbell et al., 2004; Yonezawa et al., 2005). Although there is a clear correlation between HIV-1-mediated recruitment, CD4 and co-receptor polarization, and efficient viral fusion and infection (Iyengar et al., 1998; Jolly et al., 2004; Manes et al., 2000), little is known about the molecular mechanisms regulating the CD4–co-receptor interaction. Recently, it has been reported that filamin A links HIV-1 receptors to the actin cytoskeleton to allow their clustering (Jimenez-Baranda et al., 2007).

HIV-1 viral entry occurs at specific cell-surface areas enriched in viral receptors, such as ruffles and microvilli (Singer et al., 2001; Steffens and Hope, 2003). The behavior of these structures is governed by cortical actin dynamics, which in turn depend on the activity of several actin cytoskeleton associated proteins such as those responsible for actin filament growth and capping (Mangeat et al., 1999). Ezrin-radixin-moesin (ERM) proteins provide an inducible and reversible link between membrane-associated proteins and the actin cytoskeleton (Bretscher, 1999; Mangeat et al., 1999), thereby regulating microvilli formation (Takeuchi et al., 1994). Soluble ERM proteins in the cytoplasm do not display plasma membrane and actin crosslinking capacity. This inactive state of ERM proteins is controlled by intramolecular associations between the N-terminal FERM domain (band 4.1-ezrin-radixin-moesin) and the C-terminal domain (Chishti et al., 1998; Pearson et al., 2000). ERM activation requires dissociation of these domains to facilitate other intermolecular interactions (Gary and Bretscher, 1995; Hirao et al., 1996; Matsui et al., 1998). Phosphorylation of C-terminal threonine residues in ERM (moesin Thr558 and ezrin Thr567) is indicative of the activation of the ERM molecules (Fievet et al., 2004), which in their active conformation connect cortical F-actin to the plasma membrane. The FERM domain also interacts with the cytoplasmic tails of several integral membrane proteins such as CD43, CD44, VCAM1, and ICAM1, ICAM2 and ICAM3, and mediates their cell-surface clustering (Barreiro et al., 2002; Heiska et al., 1998; Helander et al., 1996; Hirao et al., 1996; Matsui et al., 1998; Serrador et al., 1997; Takeuchi et al., 1994; Yonemura et al., 1993). The C-terminal domain of ERM molecules binds to actin filaments (Algrain et al., 1993).

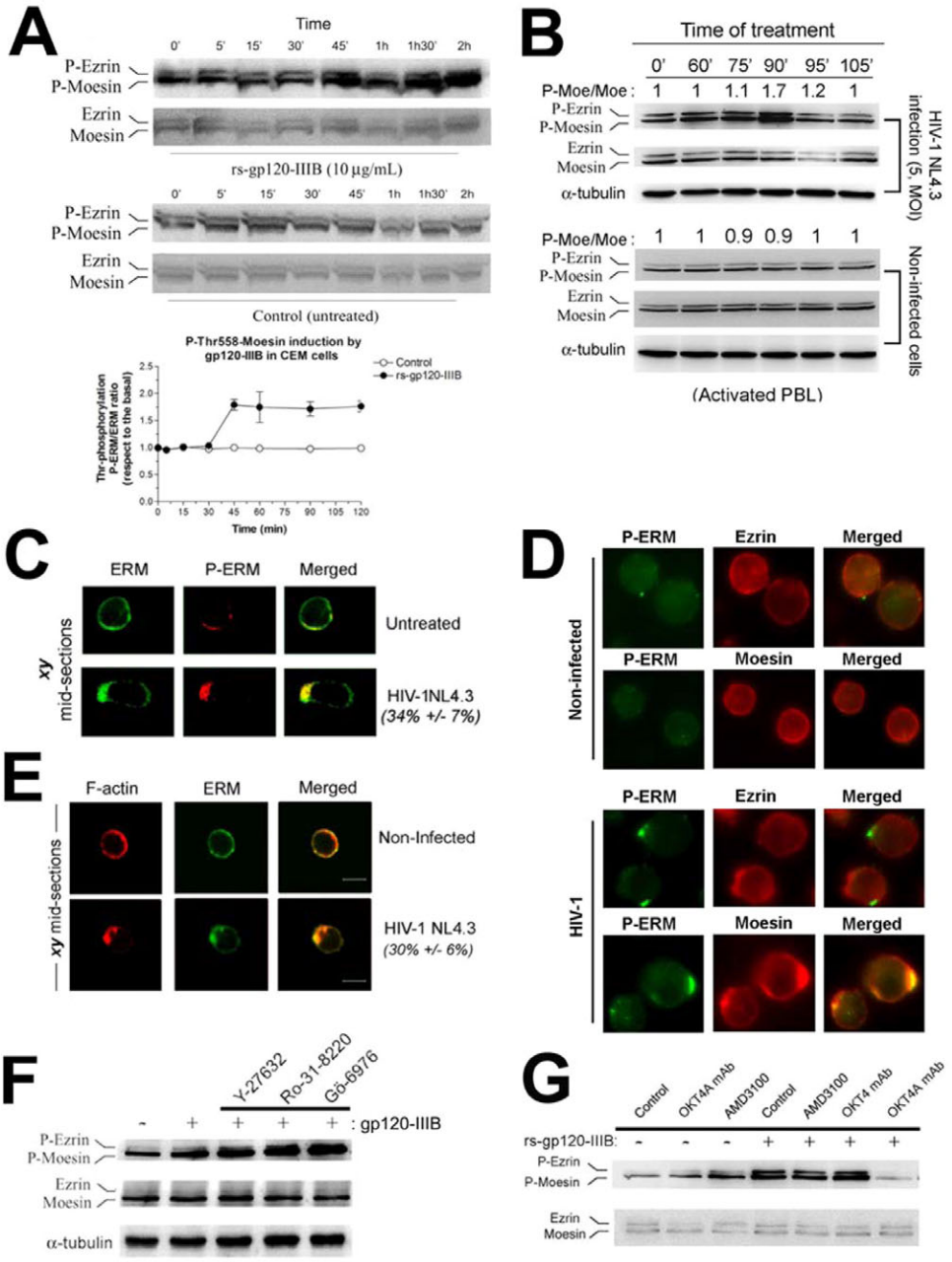

Fig. 1. HIV-1 phosphorylates endogenous ERM and redistributes F-actin. (A) Western blot analysis of rs-gp120-induced phosphorylation of C-terminal Thr residues of ERM proteins (P-ezrin and P-moesin). Results from untreated control CEM cells are shown in the blot below. Total ERM (ezrin and moesin) is shown for all experimental conditions. A representative experiment of three is shown. The graph shows quantification of Thr phosphorylation of ERMs from three independent experiments. (B) Time course of ERM Thr phosphorylation in PHA-activated PBL, during early infection with the X4-tropic HIV-$1_{NL4.3}$ viral strain (MOI, 5) compared with non-infected cells. Basal phosphorylation of endogenous ERM-Thr, total ERM and total α-tubulin expression are shown for all experimental conditions. (C) Confocal microscopy shows polarized distribution (*xy* mid-sections) of activated endogenous ERM in CEM cells, 1 hour after HIV-1 infection (MOI, 1; HIV-1NL4.3). Untreated, non-infected cells. Quantification of HIV-1-induced ERM or ERM-*P* capping is indicated ± s.d. (D) Confocal analysis of ERM-*P* and endogenous ezrin and moesin localization and redistribution in non-infected or HIV-1-infected CEM cells (1 hour; MOI, 1). (E) Confocal analysis of F-actin and endogenous ERM localization and redistribution in non-infected or HIV-1-infected CEM cells (1 hour; MOI, 1). Quantification of HIV-1-induced ERM actin capping is indicated ± s.d. (F) Western blot analysis of ezrin and moesin phosphorylation induced by rs-$gp120_{IIIB}$ (1 hour exposure) in CEM cells. Blots of total expression of ezrin, moesin and α-tubulin are also shown. Rho-K (ROCK) and PKC inhibitors failed to prevent rs-$gp120_{IIIB}$-induced Thr phosphorylation of ezrin and moesin. A representative of three independent experiments is shown. (G) Blockade of rs-$gp120_{IIIB}$ (5 µg/ml)-induced ERM Thr phosphorylation in CEM cells with neutralizing or non-neutralizing anti-CD4 mAbs (OKT4A or OKT4, respectively), or with the CXCR4 antagonist AMD3100. Blots of total ezrin and moesin proteins are shown. A representative example of three independent experiments is shown.

Analyses of HIV-1 viral preparations indicate that cleaved ezrin and moesin fragments, as well as other cytoskeletal components, are found inside the virions (Lapham et al., 1996). Recently, ezrin has been shown to have a tubulin-dependent role in HIV-1 infection (Haedicke et al., 2008). ERM proteins seem to exert pleiotropic effects on HIV-1 infection, which are dependent of the tropism of the HIV-1 viral strain (Kubo et al., 2008). Although all these data suggest a role for ERM proteins during virus budding or infection, there has been no published evidence indicating an actin-dependent role of ERM in the first steps of the viral cycle.

The data presented here show that moesin-dependent reorganization of the actin cytoskeleton is a critical feature of HIV-1 Env-mediated CXCR4-CD4 colocalization and association. Moreover, moesin activity linking the plasma membrane to actin is required for efficient HIV-1 Env-mediated membrane fusion and infection.

Results

HIV-1 Env induces ERM phosphorylation and F-actin redistribution in $CD4^+$ $CXCR4^+$ lymphocytes

It has recently been proposed that ERM proteins require phosphorylation to maintain their active state (Bretscher, 1999; Yonemura et al., 2002). To study the involvement of ERM proteins and F-actin redistribution in HIV-1 infection, we first investigated whether the HIV-1 envelope (Env) gp120 viral protein and/or HIV-1 viral particles activate ERM proteins in permissive primary lymphocytes or human leukemic CEM T cells. When CEM cells were incubated with the X4-tropic recombinant soluble (rs)-$gp120_{IIIB}$ protein, the phosphorylation of moesin, and to a lesser extent ezrin, increased (Fig. 1A, top panel), whereas total moesin and ezrin expression was unaffected (Fig. 1A, bottom panel). Remarkably, ERM proteins were also phosphorylated during early viral infection of PHA-activated primary T lymphocytes, with a

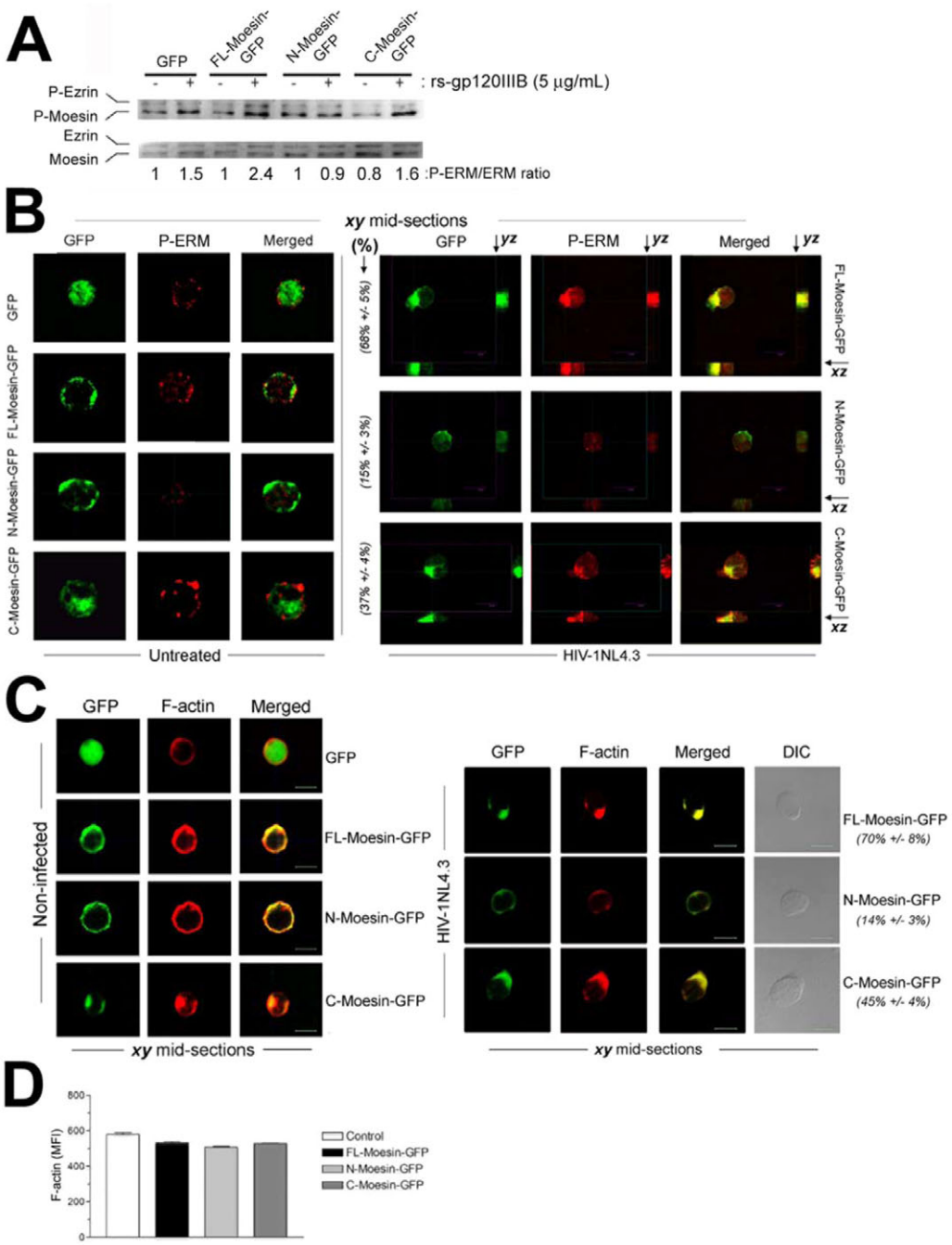

Fig. 2. F-actin and activated exogenous moesin polarize during early HIV-1 infection. (A) Western blot analysis of HIV-1 Env-induced phosphorylation of endogenous moesin in CEM cells overexpressing GFP fusions of full-length moesin (FL-moesin), the N-terminal FERM domain (N-moesin), or the C-terminal domain (C-moesin). A representative experiment is shown. ERM-*P*/ERM band density ratios from three independent experiments are shown beneath lanes. (B) ERM phosphorylation and subcellular localization of nucleofected moesin-GFP proteins in CEM cells either without infection (untreated, left panels) or 1 hour after HIV-1 infection (MOI, 1; right panels). Localization of exogenous moesin-GFP fusions was tracked by GFP fluorescence (GFP). Active ERM-*P* (Thr-*P*) was monitored with a specific Thr-*P* antibody and Alexa Fluor 568-labeled secondary antibody. The *yz* and *xz* planes are shown for each *xy* mid-section presented (arrows in the right panel). Data are from three independent experiments, presented as means ± s.e.m. Quantification of basal (untreated) and HIV-1 Env-mediated co-distribution of ERM-*P* and ERM is shown in parentheses; the percentages represent the number of cells showing co-distribution per 200 cells counted. (C) Distribution of F-actin and nucleofected moesin-GFP proteins in non-infected or HIV-1-infected (1 hour; MOI, 1) CEM cells. Quantification of HIV-1 Env-mediated co-distribution of endogenous moesin, nucleofected moesin-GFP constructs and F-actin are shown in parentheses. Scale bars: 10 µm. (D) Quantified flow cytometry of F-actin in non-infected CEM T cells that were either untransfected (Control) or nucleofected with GFP or FL-, N- or C-moesin-GFP. Data are from three independent experiments, presented as mean ± s.e.m.

peak 90 minutes after infection, which then later declined to basal levels (Fig. 1B). Confocal analysis during early HIV-1 viral exposure showed that the X4-tropic HIV-$1_{NL4.3}$ strain induces Thr phosphorylation of ERM proteins (Fig. 1C). Endogenously phosphorylated ERM displayed a polarized distribution within 1 hour of viral infection (Fig. 1C). This polarized distribution and Thr phosphorylation is mainly due to moesin, not ezrin, as indicated by the specific colocalization of moesin protein and phosphorylated threonine (Thr-*P*) (Fig. 1D). Analysis of F-actin organization showed that F-actin and endogenous moesin are cortically distributed in non-infected cells, with no capping observed (Fig. 1E), and that during early HIV-1 infection or after exposure to rs-gp120, F-actin redistributes to a pole in about 30% of cells (Fig. 1E and data not shown).

ERM C-terminal Thr residues are targets for phosphorylation in vitro by Rho kinase (ROCK) and PKC (Nakamura et al., 1999). We therefore assessed whether these kinases were responsible for the HIV-1-induced ERM phosphorylation. Phosphorylation of moesin and ezrin in response to treatment with rs-$gp120_{IIIB}$ or rs-$gp120_{SF2}$ was not affected by the specific ROCK inhibitor Y-27632 or by the PKC inhibitors Ro-31-8220 and Gö-6976 (Fig. 1F), demonstrating that HIV-1 Env-induced moesin and ezrin phosphorylation is not mediated by ROCK or PKC in lymphocytes. Moreover, neither the CXCR4 antagonist AMD3100 nor a non-neutralizing anti-CD4 OKT4 mAb affected rs-$gp120_{IIIB}$-induced moesin and ezrin phosphorylation (Fig. 1G). By contrast, pretreatment of cells with a neutralizing anti-CD4 mAb (OKT4A) abolished rs-$gp120_{IIIB}$-mediated ERM activation (Fig. 1G).

Therefore, it appears that HIV-1 Env induces moesin and ezrin phosphorylation and activation through specific CD4 engagement, ruling out the involvement of CXCR4.

Active moesin drives F-actin redistribution during initial HIV-1 to cell contacts

To further investigate the role of moesin in HIV-1 Env-mediated F-actin reorganization, we transiently nucleofected CEM cells with one of three C-terminally GFP-tagged moesin constructs: FL-moesin (full-length moesin), N-moesin (the N-terminal FERM domain), or C-moesin (the C-terminal actin-binding region) (Amieva et al., 1999). These cells were then incubated with HIV-1 viral particles. Remarkably, overexpression of functional FL-moesin increased HIV-1 Env-mediated phosphorylation of endogenous ERM (Fig. 2A), thus suggesting a cooperative effect during moesin activation (Simons et al., 1998), which could reflect enhanced anchoring of cortical F-actin filaments to plasma membrane. In non-infected cells, endogenous moesin was restricted to the cell cortex (Fig. 1E; Fig. 2B), as were exogenous FL- and N-moesin-GFP proteins (Fig. 2B, left panel). By contrast, C-moesin-GFP was detected in the cytoplasm (Fig. 2B, left panel). Interestingly, HIV-1 viral particles induced the formation of a prominent pseudopod in cells overexpressing FL-moesin or C-moesin, in which the active phosphorylated forms of moesin presented a polarized distribution (Fig. 2B, right panel). HIV-1-induced moesin redistribution and activation was not observed in CEM cells overexpressing N-moesin-GFP (Fig. 2B, right panel), which has been previously described as a dominant-negative moesin construct that lacks the capacity to bind F-actin, thereby disconnecting plasma membrane from cortical actin (Amieva et al., 1999). Moreover, the dominant-negative N-moesin construct inhibited HIV-1 Env-induced phosphorylation of endogenous moesin (Fig. 2A). These results indicate that moesin protein is activated and phosphorylated early during HIV-1 infection.

In cells overexpressing FL-moesin-GFP or C-moesin-GFP, F-actin redistribution was readily observed during HIV-1 infection or treatment with rs-gp120 viral protein (Fig. 2C, and data not shown). By contrast, N-moesin abolished HIV-1-induced F-actin redistribution (Fig. 2C). However, F-actin levels, as determined by flow cytometry (Vicente-Manzanares et al., 2004), were not altered significantly by overexpression of any of the moesin constructs (Fig. 2D). Therefore, it seems that active moesin drives F-actin redistribution during the first HIV-1 to cell contacts.

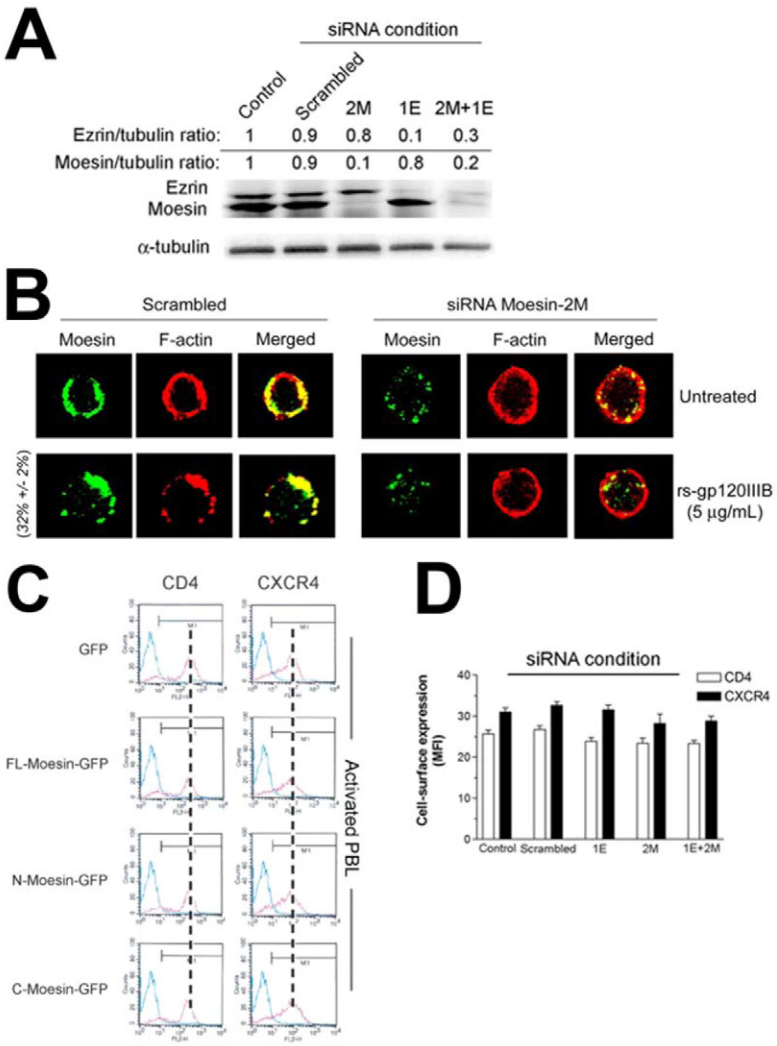

Fig. 3. Effect of overexpressed moesin-GFP proteins and moesin knockdown on CD4 and CXCR4 cell-surface levels and F-actin distribution in primary lymphocytes. (A) Western blot analysis of specific silencing of endogenous expression of ezrin (oligo 1E) and/or moesin (oligo 2M) 72 hours after siRNA nucleofection of CEM cells. Silencing of endogenous ezrin and/or moesin expression is quantified as the band intensity ratios to α-tubulin. A representative experiment of four is shown. (B) Confocal analysis of HIV-1 Env-induced F-actin redistribution in CEM cells in which endogenous moesin is suppressed by knockdown (siRNA moesin-2M). Scrambled indicates the control. *xy* mid-sections are shown. Quantification of HIV-1-induced moesin or Actin capping is indicated ± s.d. (C) CD4 and CXCR4 cell-surface expression levels (red histograms) in PHA-activated PBLs overexpressing GFP or FL-, N- or C-moesin-GFP fusion proteins. A representative flow cytometry analysis of three is shown. Blue histograms indicate IgG negative control. (D) Flow cytometry analysis of the effect of specific moesin-silencing on CD4 and CXCR4 cell surface expression in primary lymphocytes. Data are the means ± s.e.m. of four independent experiments carried out in triplicate.

Moesin regulates X4-tropic HIV-1 infection in permissive T cells

We next assessed the involvement of moesin in HIV-1 infection. We first confirmed the effect of moesin on F-actin distribution by suppressing endogenous moesin expression. Expression of ezrin, moesin or both proteins was suppressed with specific short-interfering RNAs (siRNAs) (Fig. 3A) (oligonucleotides 1E, 2M or 2M+1E; an alternative oligo for moesin was also used) (see supplementary material Fig. S1A). Knockdown of moesin expression blocked HIV-1 Env-induced F-actin redistribution (Fig. 3B). Neither overexpression of the GFP-tagged moesin constructs nor knockdown of ezrin, moesin, or both proteins affected the cell-surface expression of CD4 and CXCR4 receptors by primary lymphocytes (Fig. 3C,D).

To determine whether moesin is involved in X4-tropic HIV-1 infection, we nucleofected CEM cells or PHA-activated peripheral blood lymphocytes (PBLs) with one of the three C-terminal GFP-tagged moesin constructs and infected the cells with the X4-tropic

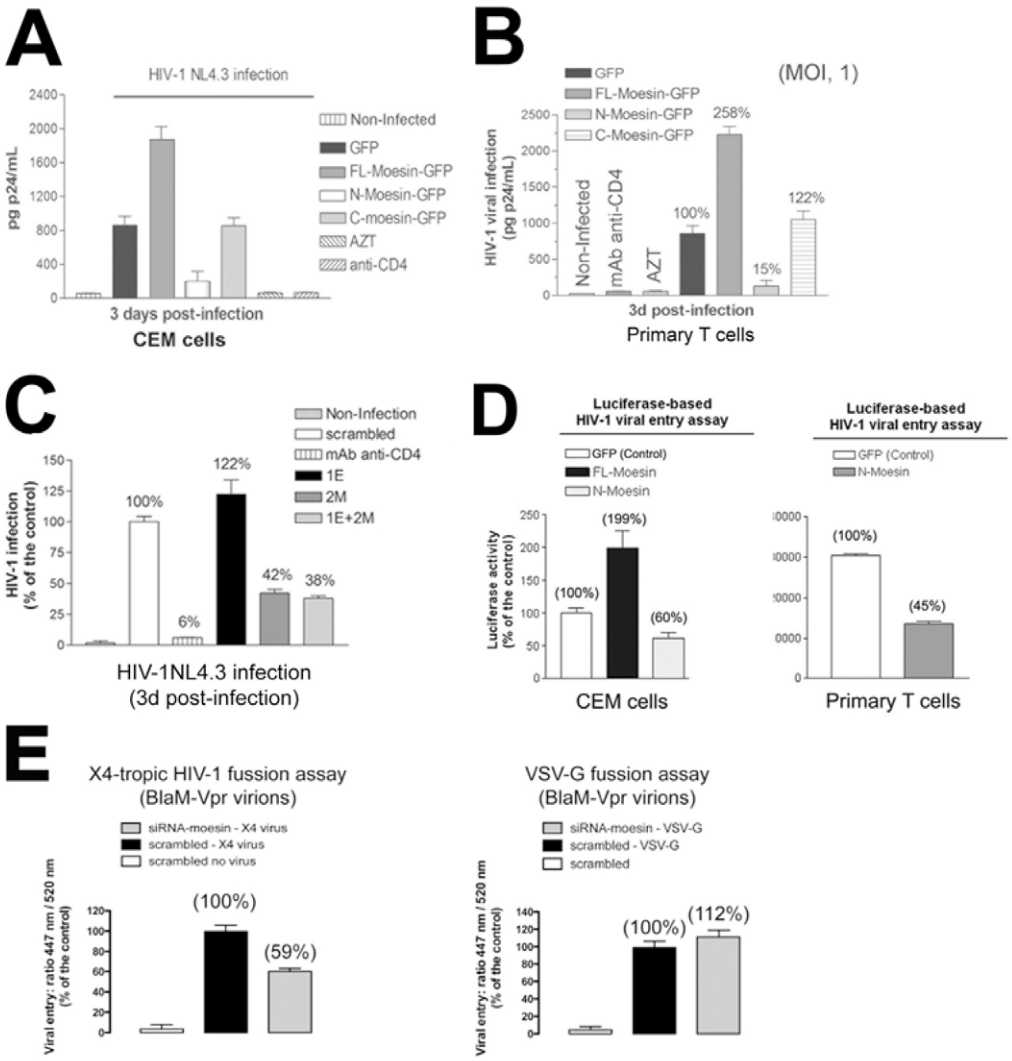

Fig. 4. Effect of overexpressed moesin-GFP proteins and moesin knockdown on HIV-1 infection and entry. (A) Effect of FL-, N- and C-moesin-GFP fusions on HIV-1 infection (MOI, 1) in CEM cells. GFP indicates transfection control for virus infection. As further controls, non-transfected cells were either not infected (non-infected) or infection was blocked with neutralizing anti-CD4 Ab (1 μg/ml) or AZT (5 μM). Data are the means ± s.e.m. of four independent experiments carried out in triplicate. (B) Effect of moesin-GFP fusions on HIV-1 infection of PHA-activated PBL (MOI, 1). GFP indicates transfection control for virus infection (defined as 100% infection). Data are the means ± s.e.m. of three independent experiments carried out in triplicate. (C) Effect of silencing endogenous ezrin and/or moesin expression on HIV-1 viral infection in CEM cells. Data are from three independent experiments carried out in triplicate, presented as means ± s.e.m. Scrambled indicates the control. When indicated, infection was inhibited with neutralizing anti-CD4 mAb. (D) Luciferase-based assay of viral entry by non-replicative HIV-1 particles in CEM T cells (left) or primary T cell blasts (right) overexpressing GFP (control, defined as 100% viral entry) or FL- or N-moesin-GFP fusions as indicated. Data are means ± s.e.m. of three independent experiments carried out in triplicate. (E) β-lactamase-based assay of viral entry by non-replicative HIV-1 particles in CEM T cells silenced for moesin (control, defined as 100% viral entry) with X4-tropic HIV-1 envelope (left panel) or VSV-G envelope (right panel). Data are means ± s.e.m. of three independent experiments carried out in triplicate.

HIV-$1_{NL4.3}$ strain. Whereas overexpression of FL-moesin strongly enhanced HIV-1 infection, the level of infection with C-moesin was similar to non-transfected or GFP-transfected permissive cells (Fig. 4A,B). CEM cells or primary T cells overexpressing the N-moesin product were less infected than controls (Fig. 4A,B). This finding was confirmed by infection of permissive moesin-silenced CEM cells; suppression of endogenous moesin, but not ezrin, inhibited HIV-1 infection (Fig. 4C; supplementary material Fig. S1B). The fact that the ezrin protein appears not to be involved in HIV-1-mediated viral infection might be explained by the low expression of this actin adaptor in T cells (Serrador et al., 1997) (and data not shown).

We next studied the involvement of moesin in the early steps of HIV-1 infection. To exclude any influence of possible effects at late steps in the infection cycle, we infected cells with a single-cycle virus bearing either the reporter gene Luciferase (Luc-HIV-1) (Gummuluru et al., 2002) or the reporter enzyme β-lactamase (Blam-HIV-1) (Cavrois et al., 2002). Non-replicative Luc-HIV-1 particles were incubated with CEM permissive cells or primary T lymphoblasts. Overexpression of FL-moesin potentiated the Luc-HIV-1 signal, whereas it was inhibited by overexpression of dominant-negative N-moesin (Fig. 4D). Therefore, the early steps of HIV-1 infection are regulated by moesin. Non-replicative Blam-HIV-1 virions were incubated with CEM permissive cells silenced

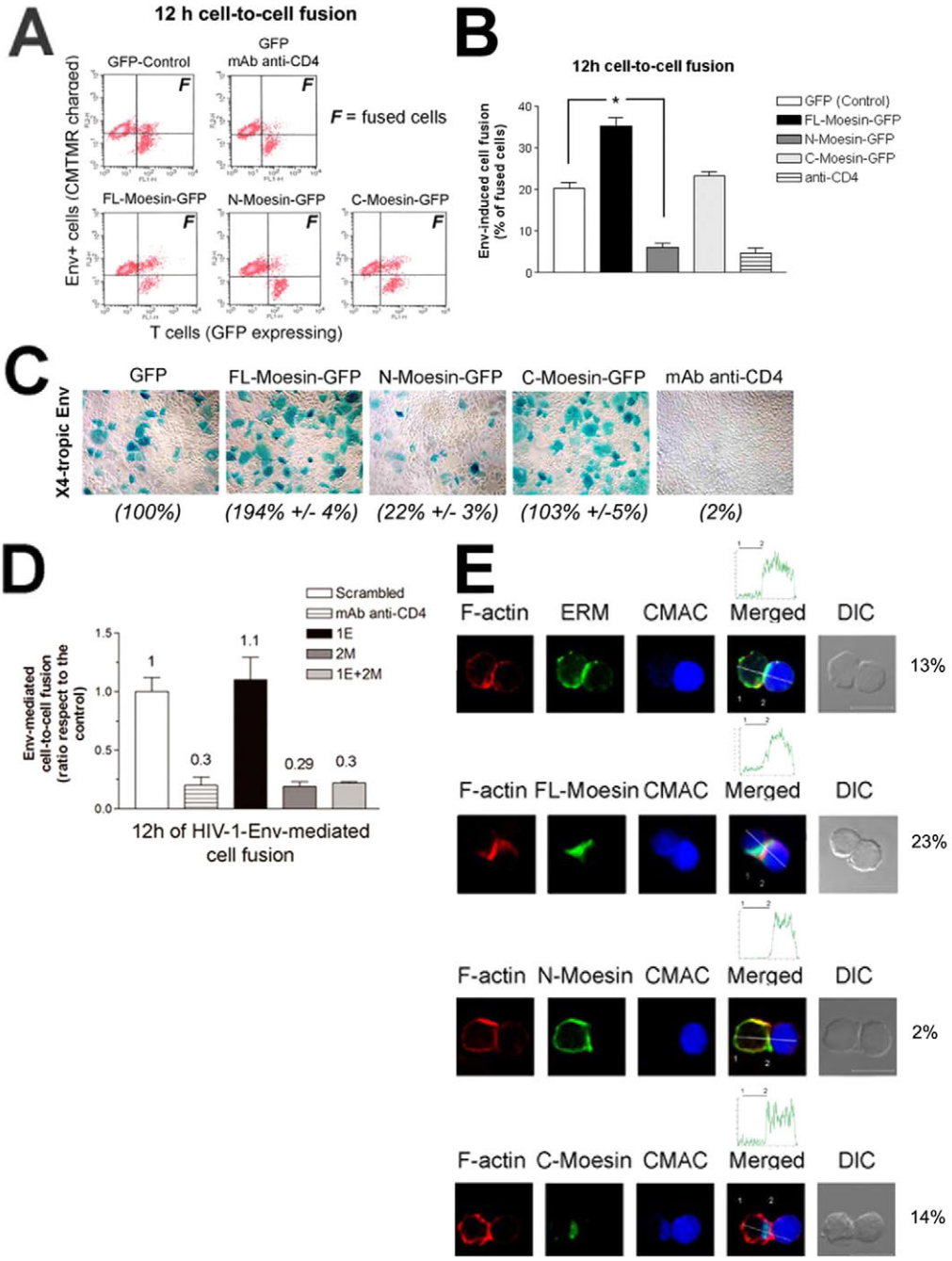

Fig. 5. Effect of moesin-GFP fusions on HIV-1 infection and HIV-1 Env-mediated cell-to-cell fusion. (A) Flow cytometry histograms show fusion (*F*) after 12 hours co-culture of Env+Jurkat-Hxbc2 cells and CEM cells overexpressing GFP (control) or FL-, N- or C-moesin-GFP fusions. A representative experiment of six is shown. (B) Quantification of six independent cell-to-cell fusion experiments as shown in A; bars show means ± s.e.m. **P*<0.01 using the Mann-Whitney U test. (C) A series of X-Gal staining showing Env-mediated membrane fusion of HeLa P4 cells, 24 hours after their lipotransfection with moesin-GFP constructs, and X4-tropic Env-HeLa 243 cells. A representative experiment of four is shown. GFP indicates transfection control for Env-induced cell fusion (100%). Quantification of three independent experiments (mean ± s.e.m., *n*=3) is shown in parentheses. (D) Effect of silencing endogenous ezrin and/or moesin on HIV-1 Env-mediated CEM-Hxbc2 cell fusion. When indicated, cell-to-cell fusion was inhibited by a neutralizing anti-CD4 mAb. Values are means ± s.e.m., *n*=4. Oligos are as indicated in Fig. 3; scrambled, non-specific RNA control sequence. (E) Confocal microscopy and quantification of Hxbc2-Env-mediated membrane fusion after 30 minutes. Localization of F-actin and endogenous ERM, and CMAC diffusion from Jurkat-derived Hxbc2 cells (blue cell to right) to the target CEM T cell (left); FL-moesin-GFP concentrates at cell-cell contacts where there is a strong accumulation of F-actin and CMAC diffuses better; N-moesin does not localize to cell contacts, impairing the redistribution of F-actin and cell-cell diffusion of CMAC; C-moesin-GFP concentrates at cell-cell contacts along with F-actin and CMAC cell-diffusion was observed. Histograms show quantification of CMAC fluorescence along the white lines (see merged pictures); segments between points 1 and 2 correspond to the cytoplasm of the target cell. The percentages represent the number of contacting cells showing redistribution per 200 cell-cell contacts counted.

for moesin to analyze the specific role of moesin in HIV-1 entry. Moesin knockdown rendered cells less susceptible to Blam-HIV-1 entry (Fig. 4E), indicating that moesin is necessary for the efficient entry of HIV-1. This process is mediated by the HIV-1 envelope because VSV-G virions penetrated equally in untreated and moesin-silenced target cells (Fig. 4E).

Moesin regulates X4-tropic HIV-1-mediated cell fusion and promotes fusion pore formation

The effect of the different moesin constructs on HIV-1-Env-dependent cell fusion was assessed in a quantitative T fusion assay, in which CEM T cells are the target for infection by Jurkat-Hxbc2 cells expressing functional X4-tropic Env. Overexpression of the N-moesin in CEM cells blocked cell fusion similarly to the neutralizing anti-CD4 mAb. By contrast, FL-moesin increased syncytia formation two- to threefold; overexpression of C-moesin did not significantly affect Env-mediated membrane fusion (Fig. 5A,B). Similar results were obtained in a HeLa-cell-based X4-tropic Env-induced fusion model (Fig. 5C).

We also assessed the involvement of ERM proteins in HIV-1 Env-mediated cell fusion by specific knockdown of lymphocyte ezrin and/or moesin protein expression. Suppression of endogenous moesin expression, but not ezrin, inhibited HIV-1 Env-mediated cell fusion (Fig. 5D).

To define the mechanism of moesin in fusion pore formation, we quantitatively assayed F-actin and moesin redistribution, as well

as dye diffusion from charged-Hxbc2-Env$^+$ cells to fused target cells. After 30 minutes, F-actin was recruited to the Env$^+$ cell-target cell contact area (Fig. 5E). ERM-*P* also accumulated in this region. Overexpression of functional FL-moesin accelerated dye diffusion from Env$^+$ cells to fused target cells, indicating enhanced membrane fusion. Moreover, F-actin recruitment to cell-cell contact areas was enhanced in cells expressing FL-moesin. By contrast, overexpression of N-moesin blocked F-actin redistribution and moesin phosphorylation at cell-cell contact areas. Moreover, N-moesin abrogated dye diffusion from Env$^+$ cells to associated T cells, indicating failure of membrane fusion. C-moesin did not affect F-actin redistribution or fusion pore formation. These results indicate that virus-activated moesin regulates an early step in HIV-1 infection by controlling fusion-pore formation, which is related to the capacity to reorganize F-actin and to promote HIV-1-Env-mediated CD4-CXCR4 interaction.

HIV-1 Env-mediated moesin activation promotes CD4-CXCR4 clustering and direct interaction

We next determined whether active moesin is involved in the HIV-1 Env-induced association of CD4-CXCR4, a process directly related to efficient viral fusion and infection (Lapham et al., 1996; Lee et al., 2000; Singer et al., 2001). The constitutive CD4-CXCR4 association (Lapham et al., 1999; Wang et al., 2004) was enhanced after gp120/CD4 engagement in CEM T cells (Fig. 6A; supplementary material Fig. S2). This gp120-induced CD4-CXCR4 association was further enhanced in cells overexpressing FL-moesin, but was blocked in cells overexpressing the dominant-negative N-moesin (Fig. 6A). CD4-CXCR4 association was also diminished in moesin-knockdown CEM T cells (Fig. 6B).

Clustering of CD4 and CXCR4 receptors during the first HIV-1 to cell contacts was assessed by confocal microscopy. HIV-1 induced an early co-distribution of CD4-CXCR4 (Fig. 6C). To further analyze how HIV-1 induces this polarization and clustering, the capping of the redistributed molecules was quantified over time by microscopy. ERMs and F-actin were the first to be recruited to the capping area, followed by CD4 and CXCR4 (Fig. 6D). Enhanced co-distribution of CD4-CXCR4 was observed in cells overexpressing FL-moesin construct (Fig. 6F), whereas the clustering in GFP-transfected cells was the same as in untransfected controls (Fig. 6E). The effect of C-moesin on receptor clustering varied in different experiments, inducing a slight enhancement of clustering (mean average 27% in C-moesin-transfected cells compared with 20% in control cells). However, no other functional effects were exerted by C-moesin in any other assays. Consistently, overexpression of N-moesin (Fig. 6E,F) or moesin mRNA silencing (Fig. 6G) impaired CD4 and CXCR4 redistribution at capping domains. Therefore, moesin regulates HIV-1-induced CD4 and CXCR4 clustering in permissive lymphocytes during the first virus-cell contacts, and this event correlates with the requirement of moesin activation for HIV-1 membrane fusion and infection.

Discussion

We have shown that HIV-1 activates endogenous ERM proteins during early viral infection. The rs-gp120 viral envelope proteins activate moesin and ezrin through interaction with CD4, but not with the CXCR4 co-receptor. Moesin phosphorylation in response to HIV-1 to T cell contact is required for cell fusion, and this is related to the capacity of phosphorylated moesin to promote CD4-CXCR4 interaction and the redistribution of F-actin and CD4-CXCR4 to sites of T-cell–virus contact. Jimenez-Baranda et al. have recently described a role for Filamin A, another actin binding protein, in the clustering of CD4-CXCR4 facilitated by the actin cytoskeleton. It is conceivable that several actin-binding proteins contribute to the regulation of transmembrane protein clustering through the actin cytoskeleton to provide the cell with the plasticity needed to respond to the environment.

The identity of the kinase responsible for moesin phosphorylation is not known. ROCK and PKC can phosphorylate ERM Thr residues in vitro (Bretscher, 1999; Nakamura et al., 1999), but the in vivo relevance of this has been controversial (Bretscher, 1999; Matsui et al., 1999; Yonemura et al., 2002). Results of the present study suggest that these kinases are not involved in HIV-1-mediated ERM phosphorylation. Increased moesin phosphorylation has been correlated with enhanced association of moesin with the cortical actin cytoskeleton (Simons et al., 1998). Moesin may thus potentiate HIV-1 Env-mediated F-actin to plasma membrane anchoring events at sites of virus to cell contact. Further studies are needed to identify the kinase or kinases that phosphorylate the C-terminal ERM-Thr in vivo in this Env-triggered CD4-signaling pathway.

Viral receptors on the surface of non-infected T cells rapidly polarize after contact with HIV-1-infected cells (Piguet and Sattentau, 2004), but the molecular signaling pathway that triggers this recruitment remains to be elucidated. The constitutive association between CD4 and CXCR4 (Lapham et al., 1999; Wang et al., 2004) is augmented after gp120-CD4 engagement. Remarkably, functional FL-moesin strongly enhanced the HIV-1 gp120-induced CD4-CXCR4 interaction and co-clustering at one pole of the lymphocyte, whereas dominant-negative N-moesin or moesin knockdown impaired this association. An important finding was that N-moesin overexpression inhibits HIV-1 Env-induced phosphorylation of endogenous moesin, thereby blocking rs-gp120- or HIV-1-induced F-actin reorganization and CD4-CXCR4 capping and interaction. Silencing of moesin impairs HIV-1 Env-mediated CD4-CXCR4 interaction, and inhibits HIV-1 viral entry and infection. By contrast, in T cells overexpressing FL-moesin, HIV-1 particles and rs-gp120 viral protein induce the formation of prominent pseudopodia, to which F-actin and CD4 and CXCR4 viral receptors redistributed. These FL-moesin-overexpressing cells were readily infected by HIV-1 replicative and non-replicative viral particles. It is thus conceivable that moesin controls the interaction of Env with CD4-CXCR4 by increasing the density of CD4-CXCR4 clusters at one pole of the cell. In turn, this would favor viral synapse and fusion-pore formation and therefore HIV-1 entry and infection.

F-actin disorganization negatively affects CD4-CXCR4 clustering and infection by X4-tropic viruses (Iyengar et al., 1998), and efficient HIV-1 viral spreading requires an intact F-actin skeleton (Jolly et al., 2007). It has recently been described that moesin and ezrin limit HIV-1 viral replication by affecting tubulin cytoskeleton at a post-entry step (Haedicke et al., 2008; Naghavi et al., 2007). Strikingly, in that study, dominant-negative N-moesin was equally as effective as the functional full-length protein at blocking viral replication, which apparently contradicts previous knowledge about how these proteins exert their function. Although the mechanism of inhibition by N-moesin, acting as a dominant negative, is not completely known, it is thought that the inhibitory activity of constructs containing only the FERM domain relies on the capacity of this domain to interact with the C-terminal regions of active endogenous ERM, thereby preventing their interaction with F-actin (reviewed by Bretscher, 1999). Therefore, when HIV-1 Env triggers moesin activation, a large fraction of the C-terminal exposed regions of endogenous moesin would be sequestered by the overexpressed

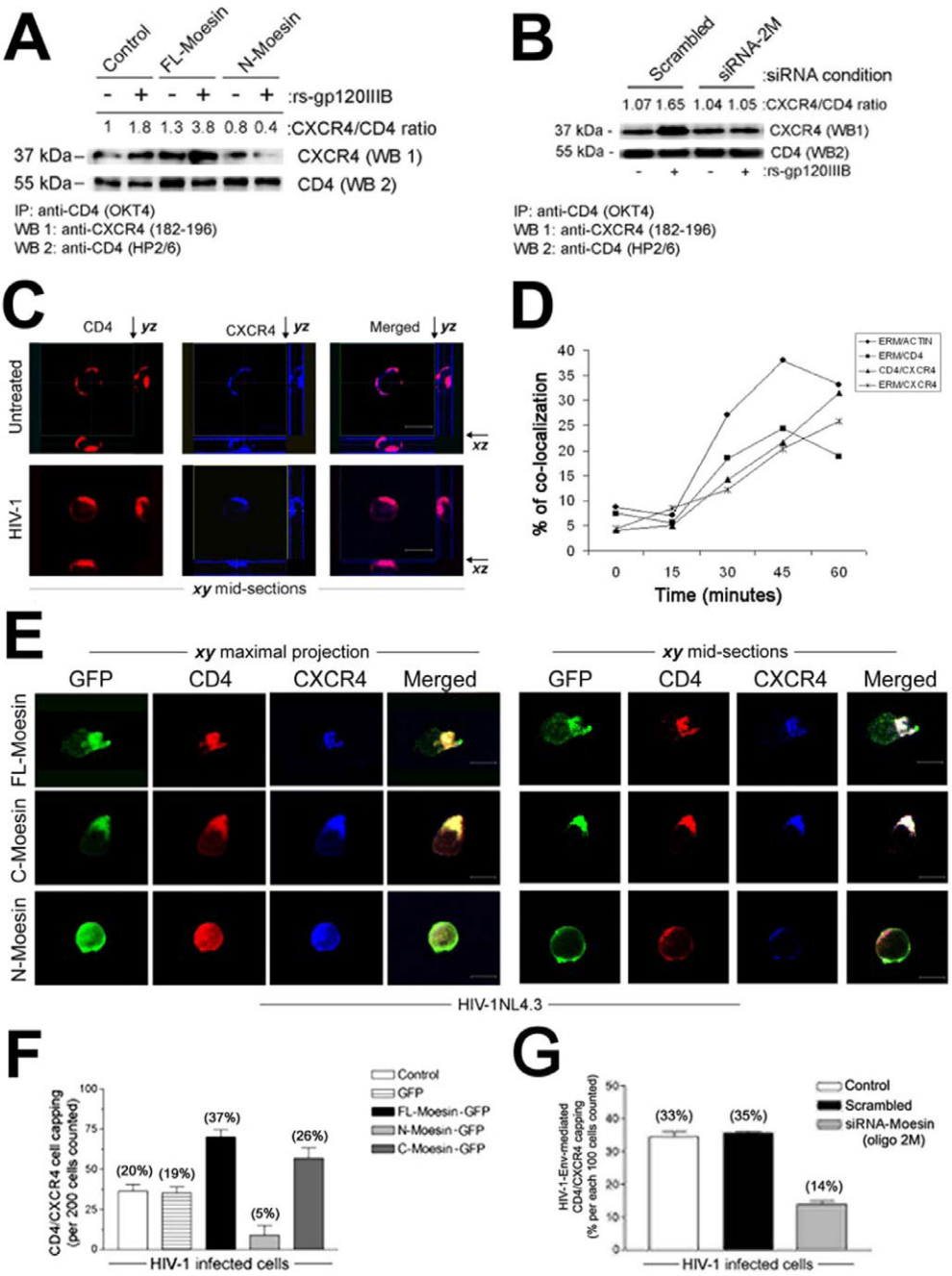

Fig. 6. Moesin drives HIV-1 Env-mediated CD4-CXCR4 interaction and polarized redistribution, during early viral infection. (A) Effect of FL- and N-moesin constructs on rs-gp120$_{IIIB}$ (10 μg/mL)-induced CD4/CXCR4 direct association. Immunoprecipitation assays were performed with anti-CD4 OKT4 mAb. Inducible co-immunoprecipitation of both receptors was measured as the ratio between the intensities of CXCR4 and CD4 immunoblotted bands. A representative experiment of three is shown. (B) Effect of the silencing of endogenous moesin on HIV-1 Env-induced direct CD4-CXCR4 interaction, in CEM cells. One representative experiment of three is shown. (C) Confocal microscopy of CD4 (anti-CD4 mAb HP2/6) and CXCR4 (biotin-conjugated mAb anti-CXCR4 12G5) in non-infected (Untreated) or 1 hour HIV-1-infected CEM cells (MOI, 1). The *yz* and *xz* planes are shown for each *xy* mid-section presented (arrows). Scale bars: 10 μm. (D) Percentage of colocalization of ERM and CD4, Actin or CXCR4, and of CD4 and CXCR4 in the presence of HIV-1 (MOI, 3) during a tim-course assay. (E) CD4 and CXCR4 redistribution in 1 hour HIV-1-infected cells overexpressing the different moesin-GFP proteins. *xy* maximal projections (left) and *xy* mid-sections (right) are shown. Scale bars: 10 μm. (F) Quantification of HIV-1-induced CD4-CXCR4 co-distribution in CEM T cells overexpressing FL-moesin-GFP and N-moesin-GFP constructs. (G) Quantification of HIV-1-induced CD4-CXCR4 capping in untransfected cells (Control), cells overexpressing the scrambled siRNA or lacking endogenous moesin (siRNA-moesin oligo 2). In F and G, quantification of HIV-1-induced CD4-CXCR4 capping is indicated as a percentage of each 200 and 100 cells counted, respectively, under each experimental condition.

FERM domain of the N-moesin construct. In agreement with our data, ERM proteins have very recently been identified as positive regulators of X4-tropic HIV-1 infection in non-lymphoid cell lines (Kubo et al., 2008). However, the molecular mechanism of the effects on HIV infection described in the study was not explored. Here, our study provides compelling evidence that ERM proteins regulate HIV-1-mediated membrane fusion and infection through the promotion of F-actin redistribution and the molecular association

and clustering of CD4 and CXCR4. Our results obtained from infection with single-cycle, non-replicative HIV-1 particles exclude effects that require late gene expression, and confirm the involvement of moesin in HIV-1 viral entry.

Our work suggests a model of moesin involvement in X4-tropic HIV-1 membrane fusion and infection of lymphocytes. In this model, HIV-1 virus activates lymphocyte moesin, as monitored by phosphorylation of Thr558. Activated moesin stabilizes and reorganizes F-actin, which may be necessary for CD4-CXCR4 colocalization at one pole of the cell. Activated moesin thus drives the HIV-1 Env-induced CD4-CXCR4 interaction. This process increases the probability of HIV-1 Env-CD4-CXCR4 interactions, potentiating fusion pore formation and thus HIV-1 viral fusion and infection. It is also conceivable that moesin-directed F-actin reorganization might drive the final steps of lipid mixing, perhaps by producing mechanical strain on the lipid bilayer (Eitzen, 2003), thus favoring viral fusion. In this regard, open-activated moesin allows F-actin anchoring in the plasma membrane, which is enhanced by FL-moesin and prevented by N-moesin. Interfering with this process inhibits HIV-1 viral fusion and infection. Therefore, the function of lymphocyte moesin is required for efficient HIV-1 viral fusion and infection.

Materials and Methods

Cells

The human $CD4^+$ $CXCR4^+$ CEM cell line was cultured in RPMI 1640 culture medium with 10% FCS. The Jurkat cell line expressing X4-tropic HIV-1-Hxbc2 Env under tetracycline-off regulation was kindly provided by the NIH-AIDS Reagent Program. Human peripheral blood lymphocytes (PBLs) were isolated from healthy donors using Ficoll-Hypaque density gradient centrifugation (GE Healthcare, Little Chalfont, UK). The PBLs were activated over 3 days with 1 μg/ml phytohemagglutinin (Murex Diagnostics, Norcross, GA), and then cultured with interleukin-2 (6 U/ml) as described (Valenzuela-Fernandez et al., 2005). The HeLa P4 cell clone, stably transfected with human CD4 cDNA and an HIV-LTR-driven β-gal reporter gene, were kindly provided by Marc Alizon (Hôpital Cochin, Paris, France). HeLa 243, also provided by M. Alizon, co-express Tat and X4-tropic Env HIV-1 proteins.

Antibodies and reagents

The anti-CD4 monoclonal antibody (mAb) HP2/6 and the non-neutralizing anti-CD4 v4-phycoerythrin mAb (PE) were previously described (Valenzuela-Fernandez et al., 2005). The neutralizing (OKT4A) and non-neutralizing (OKT4) anti-CD4 mAbs were from Ortho Diagnostic (Raritan, New Jersey). The biotin-conjugated mAb against human CXCR4 (12G5) was from Becton Dickinson Pharmingen (San Jose, CA), and anti-CXCR4 used for blots was Fusin 182-196 from Sigma (St Louis, MO). Anti-ezrin (C-19) sc-6407 is a goat polyclonal antibody (pAb) against human moesin and ezrin; and P-moesin (Thr 558) sc-12895 is a goat pAb against human moesin-*P* and ezrin-*P* at Thr558 and Thr567, respectively (Santa Cruz Biotechnology, Santa Cruz, CA). The specific anti-ezrin (4A5) sc-32759 is a mouse monoclonal antibody from Santa Cruz Biotechnology (Santa Cruz, CA). Specifc anti-moesin (38/87) ab3196 is a mouse monoclonal antibody from Abcam (Cambridge, UK). F-actin was detected with Alexa Fluor 568-labeled Phalloidin (Invitrogen, Carlsbad, CA). The anti-α-tubulin B-5-1-2 mAb and the anti-GFP pAb were from Sigma. The kinase inhibitors Ro-31-8220 (10 μM), Gö-6976 (1 μM) and Y-27632 (10 μM) were from Calbiochem (San Diego, CA). The inhibitory activity of these reagents has been tested appropriately.

Western blotting

Treated cells were resuspended in 60 μl MES buffer (10 mM MES at pH 7.4, 150 mM NaCl, 5 mM EGTA, 5 mM $MgCl_2$, 1 mM Na_3VO_4, 1 mM NaF, and a protease inhibitor cocktail (Roche Diagnostics, Mannheim, Germany), boiled for 5 minutes and immunoblotted with specific antibodies. Protein bands were analyzed using the LAS-1000 CCD system and Image Gauge 3.4 software (Fuji Photo Film Co., Tokyo, Japan).

Actin polymerization assay

Actin polymerization was analyzed as described previously (Vicente-Manzanares et al., 2004). Briefly, 24 hours after transfection, CEM T cells were fixed to stop intracellular actin polymerization with a solution containing 4% formaldehyde in PBS, 1% Triton X-100, and 5 μg/ml Alexa Fluor 647-phalloidin from Molecular Probes (Eugene, OR). Cells were incubated for 15 minutes at 37°C and washed once in PBS, and the intracellular polymerized actin was then determined with a FACScan flow cytometer (BD Biosciences, Mountain View, CA) using CellQuest software.

Immunofluorescence

Cells were fixed and permeabilized for 3 minutes in 2% formaldehyde, 0.5% Triton X-100 in PBS, and then immunostained for total ERM, P-ERM, CD4, CXCR4 or F-actin.

Moesin recombinant DNA constructs and cell transfection

Human FL-moesin-GFP, GFP-FL-moesin, N-moesin-GFP and C-moesin-GFP constructs were kindly provided by Heinz Furthmayr (Stanford University, CA) (Amieva et al., 1999). Plasmids were nucleofected into cells with Amaxa kits V (for CEM T cells) and T (for primary T cells) (Amaxa, Koeln, Germany) and transfected cells were used 24 hours after transfection. Percentages of positive nucleofected cells ranged between 40% and 70%.

HIV-1 viral preparation and infection

Preparation of HIV-$1_{NL4.3}$ and measurement of viral replication were performed as described (Valenzuela-Fernandez et al., 2005). Highly infectious preparations of HIV-$1_{NL4.3}$ viral strain were generated by several consecutive passages of the original HIV-1 isolates in peripheral blood mononuclear cells (PBMCs). Briefly, PBMCs were infected with one synchronous dose of HIV-$1_{NL4.3}$, and culture supernatants were recovered 3 days later and stored at –70°C. Freshly thawed aliquots were filtered through 0.22 μm filters before use. HIV-$1_{NL4.3}$ entry at multiplicity of infection (MOI=1) was assayed in phytohemagglutinin (PHA; 1 μg/ml)-activated PBLs or CEM T cells for 90 minutes. Cells were then trypsinized and extensively washed with fresh medium to remove viral input. Infected cells were kept in culture, and viral entry and infection was monitored every 48 hours by measuring the concentration of p24 in the culture supernatant by enzyme-linked immunosorbent assay (Innotest HIV-1 antigen mAb; Innogenetic, Ghent, Belgium). When indicated, permissive cells were pretreated with anti-CD4 mAbs (5 μg/ml) or 3′-azido-2′,3′-dideoxythymidine (AZT) (5 μg/ml) before addition of virus.

Luciferase virus assay

Luciferase-HIV-1 viral particles deficient for replication were kindly provided by Suryaram Gummuluru (Boston University, Boston, MA). Replication-deficient viral particles were produced by transfecting a luciferase-expressing reporter virus, HIV/Δnef/Δenv/luc^+, which contains the luciferase gene inserted into the *nef* ORF and does not express *env* glycoprotein (Yamashita and Emerman, 2004), with a CXCR4-tropic (Lai) *env* glycoprotein. Virus stocks were generated by PolyFect transient transfection of HEK293T cells (Gummuluru and Emerman, 2002). Two days after transfection, cell-free virus-containing supernatants were clarified of cell debris and concentrated by centrifugation (16,000 ***g*** 1 hour at 4°C) and stored at –80°C until required. HIV-1 virus preparations were titrated by ELISA and determination of the $p24^{Gag}$ content. Untreated or nucleofected CEM or PBLs activated over 2 days with PHA (1 μg/ml), were infected with a synchronous dose of luciferase-based virus for 2 hours. Virus was removed by washing infected cells. After 32 hours of infection, luciferase activity was determined with a luciferase assay kit (Promega Corporation, Madison, WI) and a 1450 Microbeta Luminescence Counter (Walax, Trilux). Protein contents were measured by the bicinchoninic acid method (BCA protein assay kit from Pierce, Rockford, IL) according to the manufacturer's instructions.

Production of non-replicative viral particles containing BlaM-Vpr

X4-tropic HIV-1 viral particles deficient for replication and containing the BlaM-Vpr chimera were produced by co-transfecting HEK293T cells with the following vectors: pNL4-3.Luc.R-E (20 μg; NIH-AIDS Reagent Program); CXCR4-tropic (HXB2-env; NIH-AIDS Reagent Program) env glycoprotein vector (10 μg) and the pCMV-BlaM-Vpr vector (10 μg). The BlaM-Vpr chimera was kindly provided by Warner C. Greene (University of California, San Francisco, CA). Co-transduction of the pNL4-3.Luc.R-E- (20 μg) vector with the pHEF-VSV-G (10 μg; NIH-AIDS Reagent Program) and pCMV-BlaM-Vpr (10 μg) vectors was used to generate non-replicative viral particles that fuse with cells in a VSV-G-dependent manner. Viral plasmids were transduced in HEK293T cells by using linear polyethylenimine with an average molecular mass of 25 kDa (PEI25k) (Polyscience, Warrington, PA). The PEI25k was prepared as a 1 mg/ml solution in water and adjusted to neutral pH. After addition of PEI25k to the viral plasmids (at a plasmid: PEI25k ratio of 1:5 w/w), the solution was mixed immediately, incubated for 20-30 minutes at room temperature and then added to HEK293T cells in culture. Viruses were harvested 40 hours after transfection. The supernatant was clarified by centrifugation at 3000 rpm for 30 minutes. Viral stocks were normalized by p24-Gag content measured by ELISA (Innogenetics, Gent, Belgium).

Virion-based fusion assay

1×10^6 CEM T permissive cells were incubated for 3 hours with equivalent viral inputs of BlaM-Vpr-containing virions (500 ng of p24) in 500 μl RPMI-1640 medium. Cells were then extensively washed to remove free virions and incubated (1 hour, room temperature) with CCF2-AM loading mix, as recommended by the manufacturer (GeneBLAzer™ detection kit; Invitrogen, Carlsbad, CA). Next, excess dye was

washed off and cells were incubated for 16 hours at room temperature prior to fixation with 4% paraformaldehyde. The percentages of cells infected were determined by measuring the fluorescence intensities of intact and cleaved CCF2 probe in virus-infected CCF2-loaded target cells in a fluorescence spectrophotometer (Cary Eclipse, Varian; Melbourne, Australia). An increase in the ratio of blue (447 nm; cleaved CCF2) to green (520 nm; intact CCF2) fluorescent signals indicates more virions fused to target cells. The background blue and green fluorescence was determined in non-infected CCF2-loaded cells (without β-lactamase activity).

CXCR4-CD4 capping assay

For capping assays, cells were co-cultured with the HIV-$1_{NL4.3}$ strain (MOI, 1) or with rs-$gp120_{IIIB}$ (5 μg/ml) for 1 hour at 37°C as described previously (Gordon-Alonso et al., 2006). Viral particles were then washed out and the cells were fixed with 2% paraformaldehyde. CD4 and CXCR4 were detected by immunofluorescence, and molecule distribution was analyzed with a Leica TCS-SP confocal microscope (Leica. Heidelberg, Germany).

CD4-CXCR4 co-immunoprecipitation

Parental or moesin-nucleofected cells were treated with rs-$gp120_{IIIB}$ (5 μg/ml) for 1 hour at 37°C. Cells were lysed at 4°C (1% CHAPS and a protease inhibitor cocktail), precleared, and incubated overnight at 4°C with anti-CD4 OKT4 mAb non-covalently complexed to protein-G-Sepharose. Co-immunoprecipitated proteins were blotted with anti-CXCR4 rabbit pAb, and reprobed after membrane stripping with HP2/6 anti-CD4 mAb.

mRNA silencing

Double-stranded siRNAs were generated against the following mRNA sequences: 5′-uccacuauguggauaauaa-3′ (1E; ezrin) 5′-agaucgaggaacagacuaa-3′ (2M; moesin) (Pust et al., 2005), (Eurogentec, Seraing, Belgium). Oligo 1M was purchased from Santa Cruz Biotechnology (moesin siRNA Ref: sc-35955). Cells were nucleofected with 1 μM siRNA and assayed 24 hours later. Irrelevant scrambled siRNA (Eurogentec) served as a control. Interference in ERM protein expression was sustained for at least 96 hours.

HIV-1 Env-mediated cell-cell fusion assays

A dual-fluorescence cell-fusion assay was also performed as described previously (Gordon-Alonso et al., 2006). Briefly, CMTMR-loaded Env+Jurkat-Hxbc2 cells were mixed with Calcein-AM-loaded parental or transfected CEM cells. The double-labeled cells were detected 6 or 12 hours later by flow cytometry. The target cells were then washed extensively to remove the drugs before co-culturing with Env-expressing cells. Anti-CD4 mAb (5 μg/ml for 30 minutes at 37°C) was used as a control for the blockage of cell fusion. The extent of fusion was calculated as the percentage fusion=(number of bound cells positive for both dyes/number of bound cells positive for calcein-labeled target cells) × 100. The β-Galactosidase and X-Gal staining cell fusion assays in the HeLa system were performed as described (Gordon-Alonso et al., 2006).

We thank M. López-Cabrera for helpful comments on the manuscript and Rafael Samaniego for confocal microscopy analyses. Editorial support was provided by S. Bartlett. This work was supported by grants BFU2005-08435/BMC, FIPSE 36289/02 (Fundación para la Investigación y Prevención del SIDA en España), Ayuda a la Investigación Básica 2002 (Fundación Juan March) and Fundación Lilly (to F.S-M.). A.V-F. was supported by grants FIPSE 24508/05, FMM (Fundación Mutua Madrileña, Spain), FIS-PI050995 from the Instituto de Salud Carlos III, Ministerio de Sanidad y Consumo, Spain, and IDT-TF-06/066 and IDT-TF-06/063 from Gobierno Autónomo de Canarias, Spain and Fondo Social Europeo (FSE; RYC2002-3018). We also thank J.M. Serrador and M. Pérez-Martinez for their support.

References

Algrain, M., Turunen, O., Vaheri, A., Louvard, D. and Arpin, M. (1993). ezrin contains cytoskeleton and membrane binding domains accounting for its proposed role as a membrane-cytoskeletal linker. *J. Cell Biol.* **120**, 129-139.

Amieva, M. R., Litman, P., Huang, L., Ichimaru, E. and Furthmayr, H. (1999). Disruption of dynamic cell surface architecture of NIH3T3 fibroblasts by the N-terminal domains of moesin and ezrin: *in vivo* imaging with GFP fusion proteins. *J. Cell Sci.* **112**, 111-125.

Barreiro, O., Yanez-Mo, M., Serrador, J. M., Montoya, M. C., Vicente-Manzanares, M., Tejedor, R., Furthmayr, H. and Sanchez-Madrid, F. (2002). Dynamic interaction of VCAM-1 and ICAM-1 with moesin and ezrin in a novel endothelial docking structure for adherent leukocytes. *J. Cell Biol.* **157**, 1233-1245.

Bretscher, A. (1999). Regulation of cortical structure by the ezrin-radixin-moesin protein family. *Curr. Opin. Cell Biol.* **11**, 109-116.

Campbell, E. M., Nunez, R. and Hope, T. J. (2004). Disruption of the actin cytoskeleton can complement the ability of Nef to enhance human immunodeficiency virus type 1 infectivity. *J. Virol.* **78**, 5745-5755.

Cavrois, M., De Noronha, C. and Greene, W. C. (2002). A sensitive and specific enzyme-based assay detecting HIV-1 virion fusion in primary T lymphocytes. *Nat. Biotechnol.* **20**, 1151-1154.

Chishti, A. H., Kim, A. C., Marfatia, S. M., Lutchman, M., Hanspal, M., Jindal, H., Liu, S. C., Low, P. S., Rouleau, G. A., Mohandas, N. et al. (1998). The FERM domain: a unique module involved in the linkage of cytoplasmic proteins to the membrane. *Trends Biochem. Sci.* **23**, 281-282.

Doms, R. W. (2000). Beyond receptor expression: the influence of receptor conformation, density, and affinity in HIV-1 infection. *Virology* **276**, 229-237.

Eitzen, G. (2003). Actin remodeling to facilitate membrane fusion. *Biochim. Biophys. Acta* **1641**, 175-181.

Fievet, B. T., Gautreau, A., Roy, C., Del Maestro, L., Mangeat, P., Louvard, D. and Arpin, M. (2004). Phosphoinositide binding and phosphorylation act sequentially in the activation mechanism of ezrin. *J. Cell Biol.* **164**, 653-659.

Gary, R. and Bretscher, A. (1995). ezrin self-association involves binding of an N-terminal domain to a normally masked C-terminal domain that includes the F-actin binding site. *Mol. Biol. Cell* **6**, 1061-1075.

Gordon-Alonso, M., Yanez-Mo, M., Barreiro, O., Alvarez, S., Munoz-Fernandez, M. A., Valenzuela-Fernandez, A. and Sanchez-Madrid, F. (2006). Tetraspanins CD9 and CD81 modulate HIV-1-induced membrane fusion. *J. Immunol.* **177**, 5129-5137.

Gummuluru, S. and Emerman, M. (2002). Advances in HIV molecular biology. *AIDS* **16 Suppl. 4**, S17-S23.

Gummuluru, S., KewalRamani, V. N. and Emerman, M. (2002). Dendritic cell-mediated viral transfer to T cells is required for human immunodeficiency virus type 1 persistence in the face of rapid cell turnover. *J. Virol.* **76**, 10692-10701.

Haedicke, J., de Los Santos, K., Goff, S. P. and Naghavi, M. H. (2008). The ERM family member ezrin regulates stable microtubule formation and retroviral infection. *J. Virol.* **82**, 4665-4670.

Heiska, L., Alfthan, K., Gronholm, M., Vilja, P., Vaheri, A. and Carpen, O. (1998). Association of ezrin with intercellular adhesion molecule-1 and -2 (ICAM-1 and ICAM-2). Regulation by phosphatidylinositol **4**, 5-bisphosphate. *J. Biol. Chem.* **273**, 21893-21900.

Helander, T. S., Carpen, O., Turunen, O., Kovanen, P. E., Vaheri, A. and Timonen, T. (1996). ICAM-2 redistributed by ezrin as a target for killer cells. *Nature* **382**, 265-268.

Hirao, M., Sato, N., Kondo, T., Yonemura, S., Monden, M., Sasaki, T., Takai, Y., Tsukita, S. and Tsukita, S. (1996). Regulation mechanism of ERM (ezrin/radixin/moesin) protein/plasma membrane association: possible involvement of phosphatidylinositol turnover and Rho-dependent signaling pathway. *J. Cell Biol.* **135**, 37-51.

Iyengar, S., Hildreth, J. E. and Schwartz, D. H. (1998). Actin-dependent receptor colocalization required for human immunodeficiency virus entry into host cells. *J. Virol.* **72**, 5251-5255.

Jimenez-Baranda, S., Gomez-Mouton, C., Rojas, A., Martinez-Prats, L., Mira, E., Ana Lacalle, R., Valencia, A., Dimitrov, D. S., Viola, A., Delgado, R. et al. (2007). Filamin-A regulates actin-dependent clustering of HIV receptors. *Nat. Cell Biol.* **9**, 838-846.

Jolly, C., Kashefi, K., Hollinshead, M. and Sattentau, Q. J. (2004). HIV-1 cell to cell transfer across an Env-induced, actin-dependent synapse. *J. Exp. Med.* **199**, 283-293.

Jolly, C., Mitar, I. and Sattentau, Q. J. (2007). Requirement for an intact T-cell actin and tubulin cytoskeleton for efficient assembly and spread of human immunodeficiency virus type 1. *J. Virol.* **81**, 5547-5560.

Kubo, Y., Yoshii, H., Kamiyama, H., Tominaga, C., Tanaka, Y., Sato, H. and Yamamoto, N. (2008). ezrin, Radixin, and moesin (ERM) proteins function as pleiotropic regulators of human immunodeficiency virus type 1 infection. *Virology* **375**, 130-140.

Kuhmann, S. E., Platt, E. J., Kozak, S. L. and Kabat, D. (2000). Cooperation of multiple CCR5 coreceptors is required for infections by human immunodeficiency virus type 1. *J. Virol.* **74**, 7005-7015.

Lapham, C. K., Ouyang, J., Chandrasekhar, B., Nguyen, N. Y., Dimitrov, D. S. and Golding, H. (1996). Evidence for cell-surface association between fusin and the CD4-gp120 complex in human cell lines. *Science* **274**, 602-605.

Lapham, C. K., Zaitseva, M. B., Lee, S., Romanstseva, T. and Golding, H. (1999). Fusion of monocytes and macrophages with HIV-1 correlates with biochemical properties of CXCR4 and CCR5. *Nat. Med.* **5**, 303-308.

Lee, S., Lapham, C. K., Chen, H., King, L., Manischewitz, J., Romantseva, T., Mostowski, H., Stantchev, T. S., Broder, C. C. and Golding, H. (2000). Coreceptor competition for association with CD4 may change the susceptibility of human cells to infection with T-tropic and macrophagetropic isolates of human immunodeficiency virus type 1. *J. Virol.* **74**, 5016-5023.

Manes, S., del Real, G., Lacalle, R. A., Lucas, P., Gomez-Mouton, C., Sanchez-Palomino, S., Delgado, R., Alcami, J., Mira, E. and Martinez, A. C. (2000). Membrane raft microdomains mediate lateral assemblies required for HIV-1 infection. *EMBO Rep.* **1**, 190-196.

Mangeat, P., Roy, C. and Martin, M. (1999). ERM proteins in cell adhesion and membrane dynamics. *Trends Cell Biol.* **9**, 187-192.

Matsui, T., Maeda, M., Doi, Y., Yonemura, S., Amano, M., Kaibuchi, K., Tsukita, S. and Tsukita, S. (1998). Rho-kinase phosphorylates COOH-terminal threonines of ezrin/radixin/moesin (ERM) proteins and regulates their head-to-tail association. *J. Cell Biol.* **140**, 647-657.

Matsui, T., Yonemura, S., Tsukita, S. and Tsukita, S. (1999). Activation of ERM proteins in vivo by Rho involves phosphatidyl-inositol 4-phosphate 5-kinase and not ROCK kinases. *Curr. Biol.* **9**, 1259-1262.

Naghavi, M. H., Valente, S., Hatziioannou, T., de Los Santos, K., Wen, Y., Mott, C., Gundersen, G. G. and Goff, S. P. (2007). moesin regulates stable microtubule formation and limits retroviral infection in cultured cells. *EMBO J.* **26**, 41-52.

Nakamura, F., Huang, L., Pestonjamasp, K., Luna, E. J. and Furthmayr, H. (1999). Regulation of F-actin binding to platelet moesin *in vitro* by both phosphorylation of threonine 558 and polyphosphatidylinositides. *Mol. Biol. Cell* **10**, 2669-2685.

Pearson, M. A., Reczek, D., Bretscher, A. and Karplus, P. A. (2000). Structure of the ERM protein moesin reveals the FERM domain fold masked by an extended actin binding tail domain. *Cell* **101**, 259-270.

Piguet, V. and Sattentau, Q. (2004). Dangerous liaisons at the virological synapse. *J. Clin. Invest.* **114**, 605-610.

Pontow, S. E., Heyden, N. V., Wei, S. and Ratner, L. (2004). Actin cytoskeletal reorganizations and coreceptor-mediated activation of rac during human immunodeficiency virus-induced cell fusion. *J. Virol.* **78**, 7138-7147.

Pust, S., Morrison, H., Wehland, J., Sechi, A. S. and Herrlich, P. (2005). Listeria monocytogenes exploits ERM protein functions to efficiently spread from cell to cell. *EMBO J.* **24**, 1287-1300.

Serrador, J. M., Alonso-Lebrero, J. L., del Pozo, M. A., Furthmayr, H., Schwartz-Albiez, R., Calvo, J., Lozano, F. and Sanchez-Madrid, F. (1997). moesin interacts with the cytoplasmic region of intercellular adhesion molecule-3 and is redistributed to the uropod of T lymphocytes during cell polarization. *J. Cell Biol.* **138**, 1409-1423.

Simons, P. C., Pietromonaco, S. F., Reczek, D., Bretscher, A. and Elias, L. (1998). C-terminal threonine phosphorylation activates ERM proteins to link the cell's cortical lipid bilayer to the cytoskeleton. *Biochem. Biophys. Res. Commun.* **253**, 561-565.

Singer, II, Scott, S., Kawka, D. W., Chin, J., Daugherty, B. L., DeMartino, J. A., DiSalvo, J., Gould, S. L., Lineberger, J. E., Malkowitz, L. et al. (2001). CCR5, CXCR4, and CD4 are clustered and closely apposed on microvilli of human macrophages and T cells. *J. Virol.* **75**, 3779-3790.

Steffens, C. M. and Hope, T. J. (2003). Localization of CD4 and CCR5 in living cells. *J. Virol.* **77**, 4985-4991.

Takeuchi, K., Sato, N., Kasahara, H., Funayama, N., Nagafuchi, A., Yonemura, S., Tsukita, S. and Tsukita, S. (1994). Perturbation of cell adhesion and microvilli formation by antisense oligonucleotides to ERM family members. *J. Cell Biol.* **125**, 1371-1384.

Valenzuela-Fernandez, A., Alvarez, S., Gordon-Alonso, M., Barrero, M., Ursa, A., Cabrero, J. R., Fernandez, G., Naranjo-Suarez, S., Yanez-Mo, M., Serrador, J. M. et al. (2005). Histone deacetylase 6 regulates human immunodeficiency virus type 1 infection. *Mol. Biol. Cell* **16**, 5445-5454.

Vicente-Manzanares, M., Viton, M. and Sanchez-Madrid, F. (2004). Measurement of the levels of polymerized actin (F-actin) in chemokine-stimulated lymphocytes and GFP-coupled cDNA transfected lymphoid cells by flow cytometry. *Methods Mol. Biol.* **239**, 53-68.

Wang, J., Alvarez, R., Roderiquez, G., Guan, E. and Norcross, M. A. (2004). Constitutive association of cell surface CCR5 and CXCR4 in the presence of CD4. *J. Cell Biochem.* **93**, 753-760.

Yamashita, M. and Emerman, M. (2004). Capsid is a dominant determinant of retrovirus infectivity in nondividing cells. *J. Virol.* **78**, 5670-5678.

Yonemura, S., Nagafuchi, A., Sato, N. and Tsukita, S. (1993). Concentration of an integral membrane protein, CD43 (leukosialin, sialophorin), in the cleavage furrow through the interaction of its cytoplasmic domain with actin-based cytoskeletons. *J. Cell Biol.* **120**, 437-449.

Yonemura, S., Matsui, T., Tsukita, S. and Tsukita, S. (2002). Rho-dependent and -independent activation mechanisms of ezrin/radixin/moesin proteins: an essential role for polyphosphoinositides *in vivo*. *J. Cell Sci.* **115**, 2569-2580.

Yonezawa, A., Cavrois, M. and Greene, W. C. (2005). Studies of ebola virus glycoprotein-mediated entry and fusion by using pseudotyped human immunodeficiency virus type 1 virions: involvement of cytoskeletal proteins and enhancement by tumor necrosis factor alpha. *J. Virol.* **79**, 918-926.